SUPPORTING INFORMATION

Anions-induced changes of structure interpenetration and magnetic property in 3D Dy-Cu metal-organic frameworks†

Peng-Fei Shi, Gang Xiong, Bin Zhao,* Zhan-Yun Zhang, and Peng Cheng*

Department of Chemistry, Key Laboratory of Advanced Energy Material Chemistry, MOE, and TKL of Metal and Molecule Based Material Chemistry, Nankai University, Tianjin 300071, China. Fax: (+86)-22-23502458 E-mail: zhaobin@nankai.edu.cn

Materials and General Characterizations

All of the chemicals are analytically grade and purchased without further purification. Elemental analyses for C, H, and N were obtained at the Institute of Elemental Organic Chemistry, Nankai University. The FT-IR spectrum was measured with a Bruker Tensor 27 Spectrophoto meter on KBr disks. TGA experiments were performed on a NETZSCH TG 209 instrument with a heating rate of 10 ℃ min^{-1}. Powder X-ray Diffraction measurements were recorded on a D/Max-2500 X-ray Diffractometer using Cu-Kα radiation. The magnetic properties were measured on a Quantum Design MPMS-XL7 and a PPMS-9 ACMS magnetometer. Diamagnetic correction was made with Pascal's constants for all the constituent atoms.

Synthesis of 1 and 2

Compound **1**: A mixture of H_2BPDC (0.0488 g, 0.15 mmol), $CuCl_2·6H_2O$ (0.0123 g, 0.05 mmol), $DyCl_3·6H_2O$ (0.0377 g, 0.1 mmol), 4 mL distilled water and 4 mL anhydrous alcohol were sealed in a Teflon-lined stainless vessel (25 mL) and heated at 145℃ for 72 h under autogenous pressure. The vessel was then cooled slowly down to room temperature at 1.2 ℃/ h. Blue block crystals were obtained. The yield was 62% (based on $DyCl_3·6H_2O$). Elemental Anal. (%) Calcd: C, 35.44; H, 2.42; N: 6.89. Found: C, 35.26; H, 2.19; N: 6.54.

Compound **2**: A mixture of H_2BPDC (0.0366 g, 0.15 mmol), $Cu(NO_3)_2·6H_2O$ (0.0148 g, 0.05 mmol), $Dy(NO_3)_3·6H_2O$ (0.0456 g, 0.1 mmol), 4 mL distilled water and 4 mL anhydrous alcohol were sealed in a Teflon-lined stainless vessel (25 mL) and heated at 145℃ for 72 h under autogenous pressure. The vessel was then cooled slowly down to

room temperature at 1.2 ℃/ h. Blue needlelike crystals were obtained. The yield was 45% (based on $Dy(NO_3)_3{\cdot}6H_2O$). Elemental Anal. (%) Calcd: C, 29.00; H, 3.11; N: 7.51. Found: C, 28.79; H, 3.40; N: 7.65.

Crystallographic Studies

Crystallographic data of **1** and **2** were collected on a SuperNova single crystal diffractometer equipped with graphite-monochromatic MoKα radiation (λ = 0.71073 Å). The data integration and empirical absorption corrections were carried out by SAINT programs. The structures were solved by direct methods. All the non-hydrogen atoms were refined anisotropically on F^2 by full-matrix least-squares techniques. All hydrogen atoms except for those of the uncoordinated water molecules in these coordination polymers were generated geometrically and refined isotropically using the riding model.

Additionally, due to low residual electron density, the positions of NO_3^- and H_2O in compound **2** cannot be determined accurately by single crystal X-ray diffraction techniques, and therefore the SQUEEZE routine in the PLATON software package was applied. This method was widely applied in the previous articles (For example: *Science* **2010**, *329*, 1053). For compound **2**, the squeezed electron number is 739 for four units, which is consistent with two NO_3^- and twelve free H_2O [4*(2*32+12*10) = 736]. Simultaneously, the elemental analyses of C, H, and N are close to that of calculated according to the molecular formula mentioned above.

Structures of 1 and 2

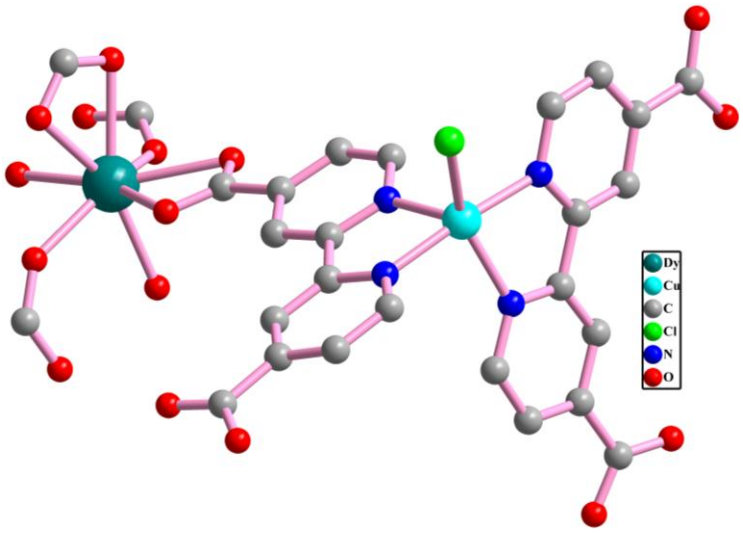

Fig. S1 The coordination environments of Dy^{3+}, Cu^{2+} and $BPDC^{2-}$ ligands in compound **1**.

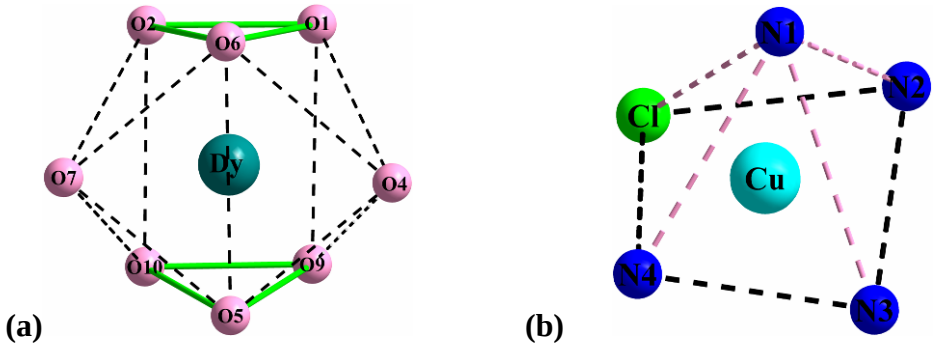

Fig. S2 (a) The dicapped trigonal prism geometry of Dy^{3+} in compound **1**; (b) the square pyramid geometry of Cu^{2+} in compound **1**.

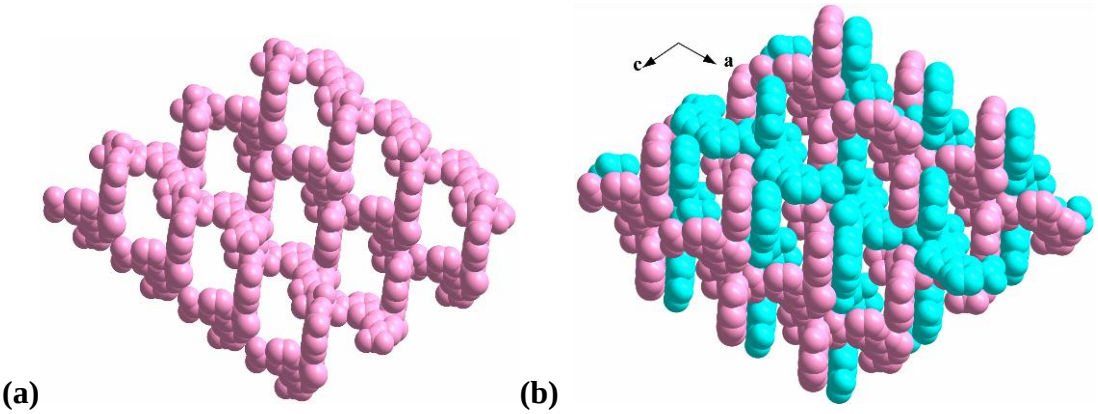

Fig. S3 (a) One set of the two-fold interpenetration along the *b* direction in compound **1**; (b) the two-fold interpenetration along the *b* direction in compound **1**.

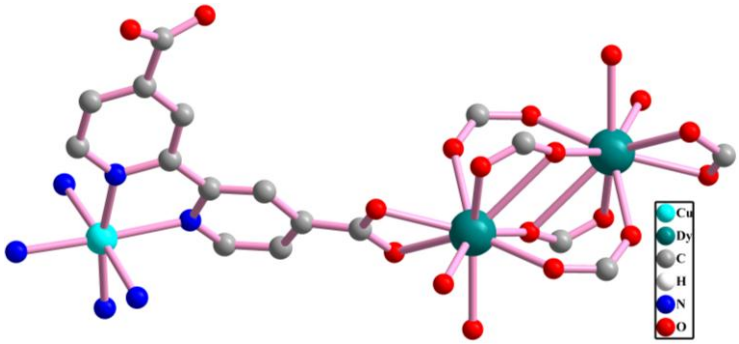

Fig. S4 The coordination environments of Dy^{3+}, Cu^{2+} and $BPDC^{2-}$ ligands in compound **2**.

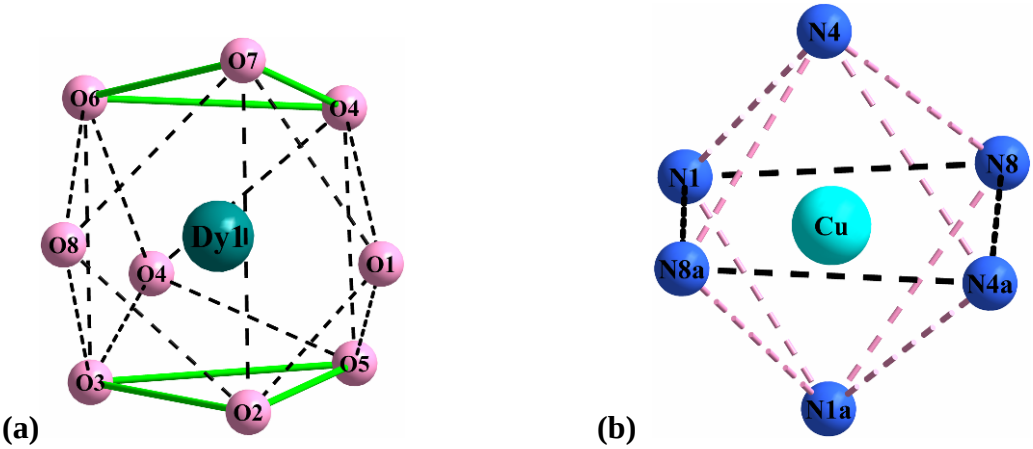

Fig. S5 (a) The tricapped trigonal prism geometry of Dy^{3+} in compound **2**; (b) the octahedral geometry of Cu^{2+} in compound **2**.

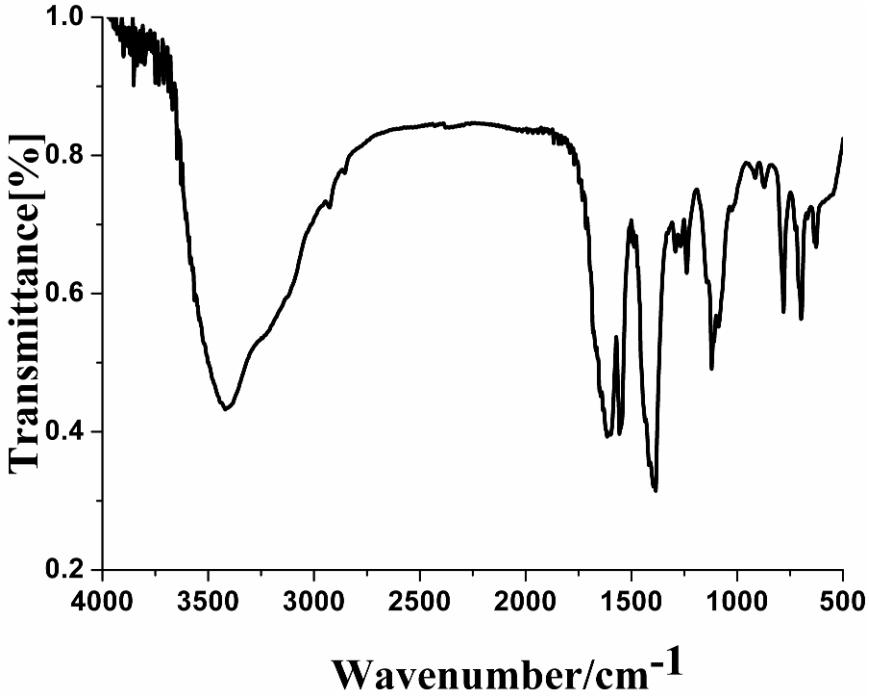

Fig. S6 FT-IR of compound **2**.

Powder X-ray Diffraction (PXRD) and Thermogravimetric analyses (TGA)

The PXRD patterns of **1** and **2** are in conformity with the simulated that from the single crystal data of **1** and **2**, respectively (Fig. S5, S6), which prove the purity of the samples.

To study the thermal stability of the two compounds and further affirm the molecular formula of the compound **2**, thermogravimetric analyses of **1** and **2** were detected in the range of 25-800 ℃, as shown in Fig. S7. The TGA curve of **1** exhibits three regions of weight loss. The first weight loss between 25 and 125℃ is 3.54%, and it corresponds to the loss of one and three quarters water molecules, being identical with the calculated 3.87%. The second weight loss between 125 and 310 ℃ is 4.78%, and it corresponds to the loss of two coordinated water molecules, being identical with the calculated 4.42%. The third weight loss above 310 ℃ stems from the decomposition of the 3D framework in **1**. For compound **2**, the first weight loss from the room temperature to 300 ℃ is 18.36%, and it corresponds to four coordinated and twelve free water molecules, which is well consistent with the calculated value 18.88%. Upon increasing the temperature, the framework commences to collapse.

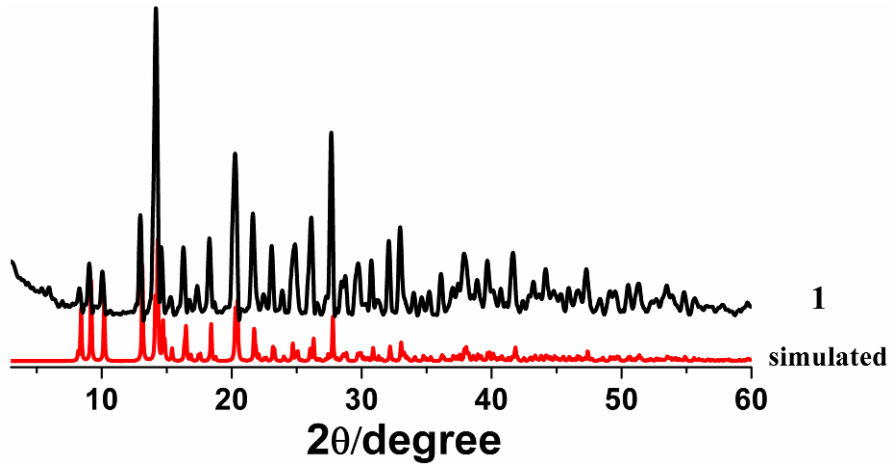

Fig. S7 PXRD patterns of compound **1** and the simulated one of **1**.

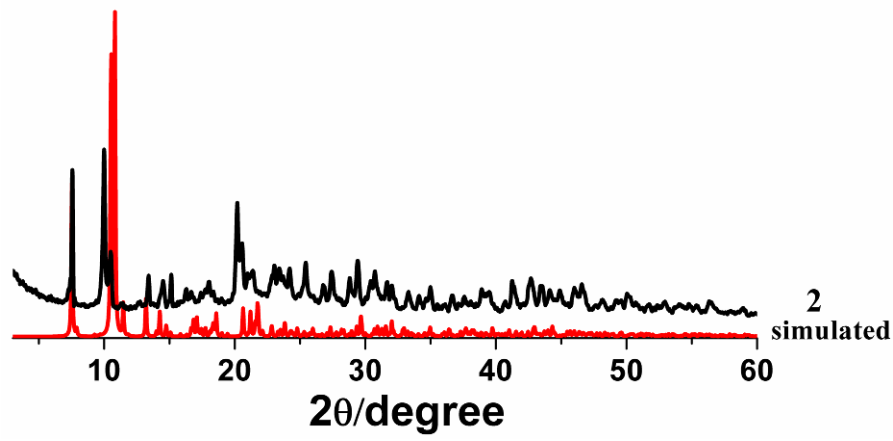

Fig. S8 PXRD patterns of compound **2** and the simulated one of **2**.

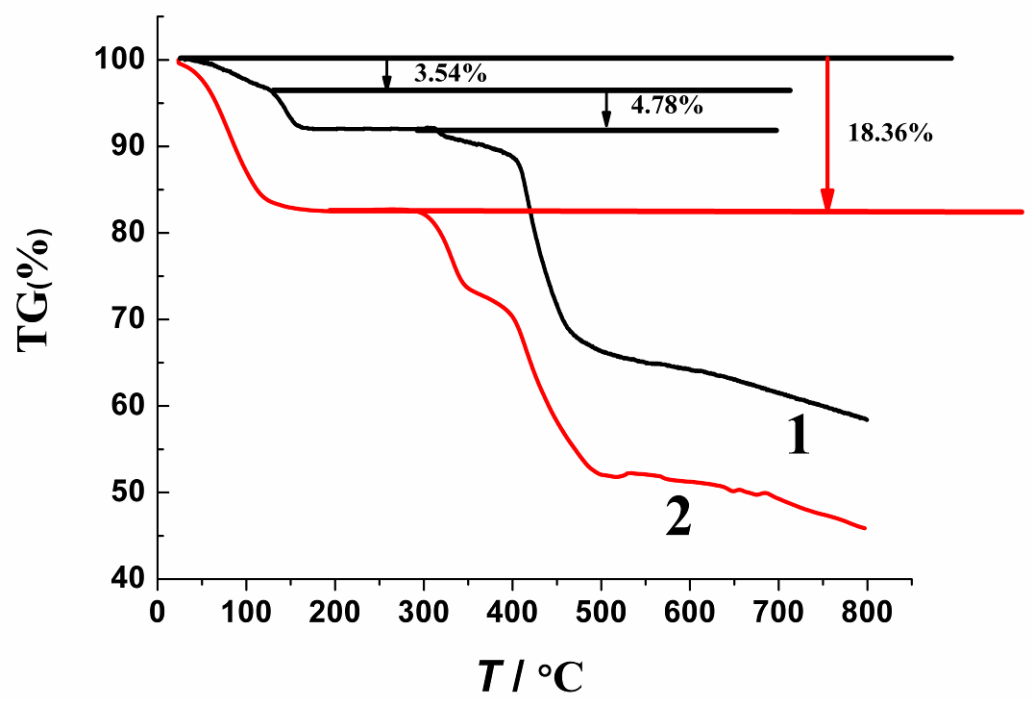

Fig. S9 TGA cures of compounds **1** and **2**.

For most of lanthanide ions, due to the large orbital-angular momentum, strong spin-orbital coupling, and very weak magnetic interaction between adjacent lanthanide ions originated from the nature of inner 4*f* electrons, it is rather difficult to fit the magnetic data of the compounds containing Ln^{3+} based on accurate theoretical equation. However, for Dy2 dimer system, Dy^{3+} in a very low-temperature region can be approximately considered as an ion with an effective spin $S = 1/2$ and large anisotropic g tensor, and thus the $\chi_M T$ vs T plots can be fitted by the mathematical equation: $(Ng^2\beta^2/3k)\ [1+\exp(-J/2kT)]^{-1}$ (*Chem.*

Eur. J. 2011, 17, 10397-10404). For compound **2**, the $\chi_M T$ vs T plots were fitted by the dimer Ising model $\chi_M T = (Ng^2\beta^2/3k)\ [1+\exp(-J/2kT)]^{-1} + 0.375$ (0.375 = $(Ng^2\beta^2/3k)*S(S+1)$, which is the contribution of one isolated Cu^{2+}) in the temperature range between 4 and 11 K with the results of $J = -0.58$ cm^{-1} and $g =$ 19.98 (Fig. S10), but the data between 2 and 4 K can not be fitted. Compared with compound **2**, compound **1** possesses a longer distance of $Dy^{3+}\ldots Dy^{3+}$ with 6.0907(6) Å. Thus, the magnetic data was dealt with by magnetic unit including two Dy^{3+} and two Cu^{2+}, and the $\chi_M T$ vs T plots were also tried to be fitted by the dimer Ising model above $\chi_M T = (Ng^2\beta^2/3k)\ [1+\exp(-J/2kT)]^{-1} + 0.75$ (0.75 is the contribution of two isolated Cu^{2+}) in the low temperature range between 2 and 8 K, yielding $J = -0.25$ cm^{-1} and $g = 20.02$ (Fig. S10). The g value in **1** and **2** falls into a normal range, and the smaller exchange energy (J) in **1** than that in **2** may originate from the long distance (6.09 Å) between adjacent Dy^{3+} in **1**.

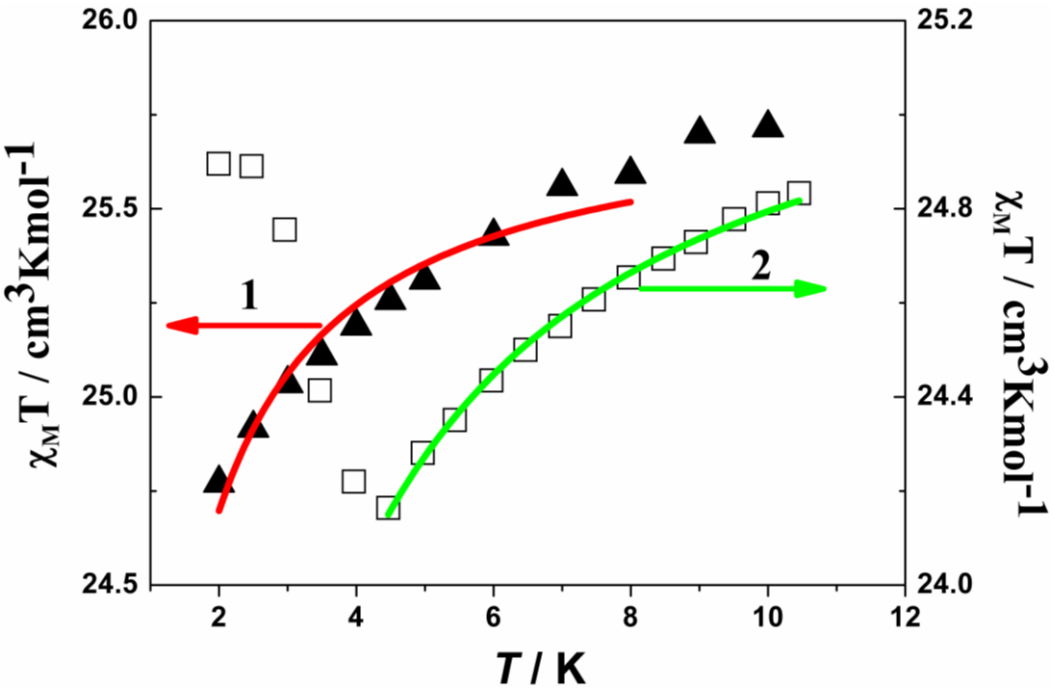

Fig. S10 Temperature dependence of $\chi_M T$ in the range of 2−10 K for compound **1** (▲) and **2** (□), and the best fit using the dimer Ising model: 2−8 K for compound **1** (red line), 4-10 K for compound **2** (green line).

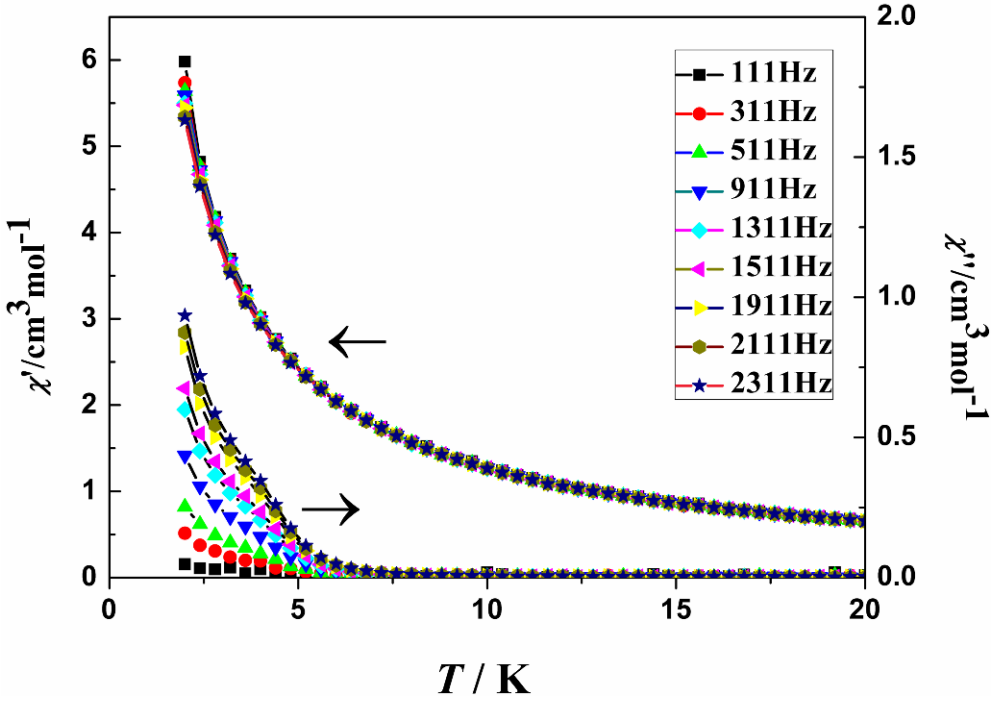

Fig. S11 Temperature dependence of the in phase and out-of-phase signals of the ac susceptibility for **1** (H_{ac} = 3 Oe, H_{dc} = 0 Oe). Solid lines are guides for the eye.

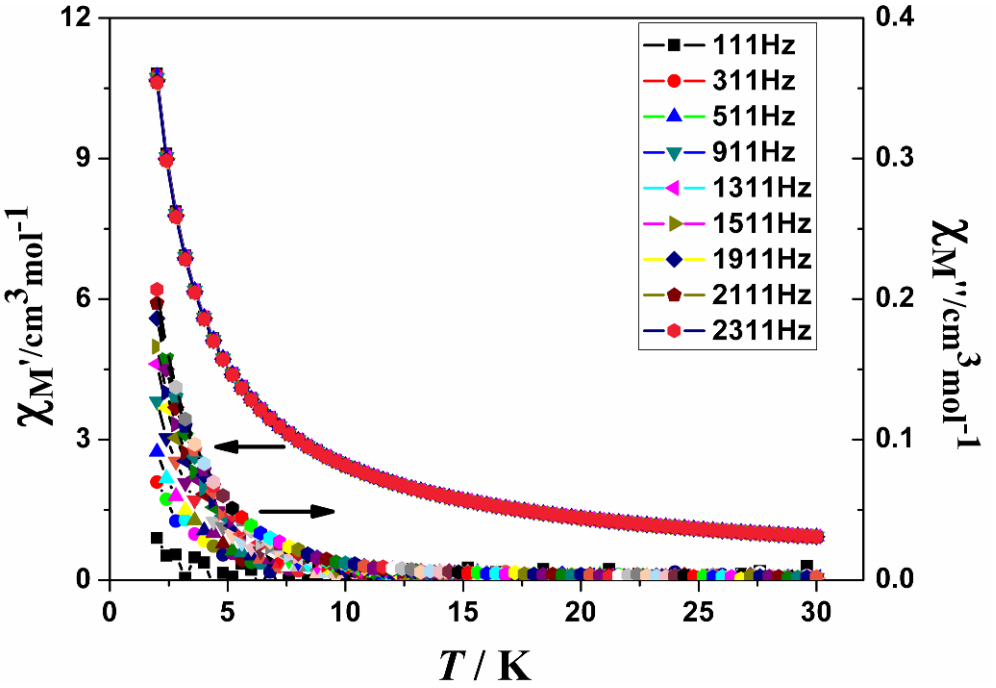

Fig. S12 Temperature dependence of the in phase and out-of-phase signals of the ac susceptibility for **2** (H_{ac} = 3 Oe, H_{dc} = 0 Oe). Solid lines are guides for the eye.

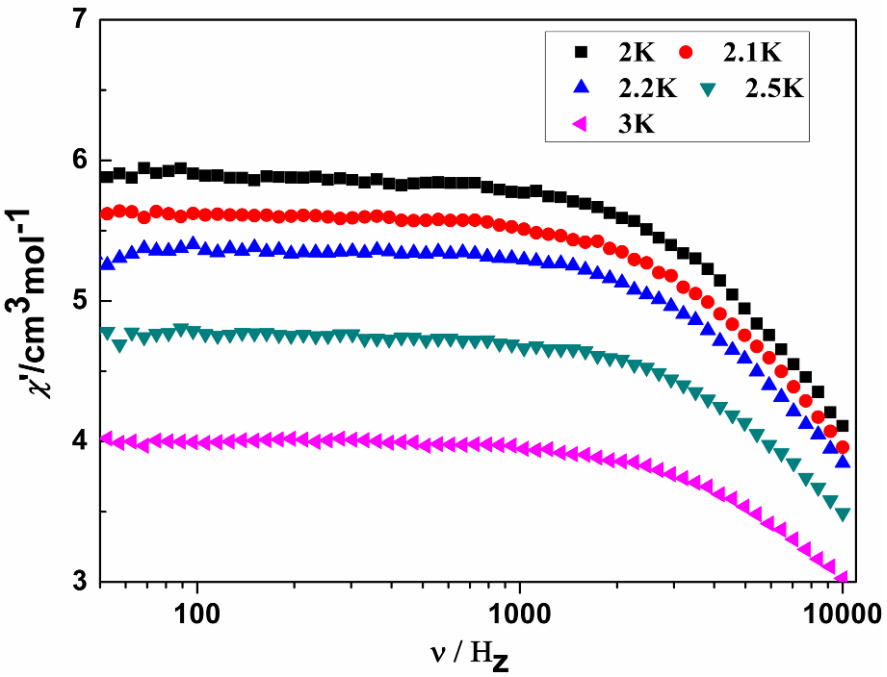

Fig. S13 Frequency dependence of the in phase signals of the ac susceptibility for **1** at H_{dc} = 0 Oe.

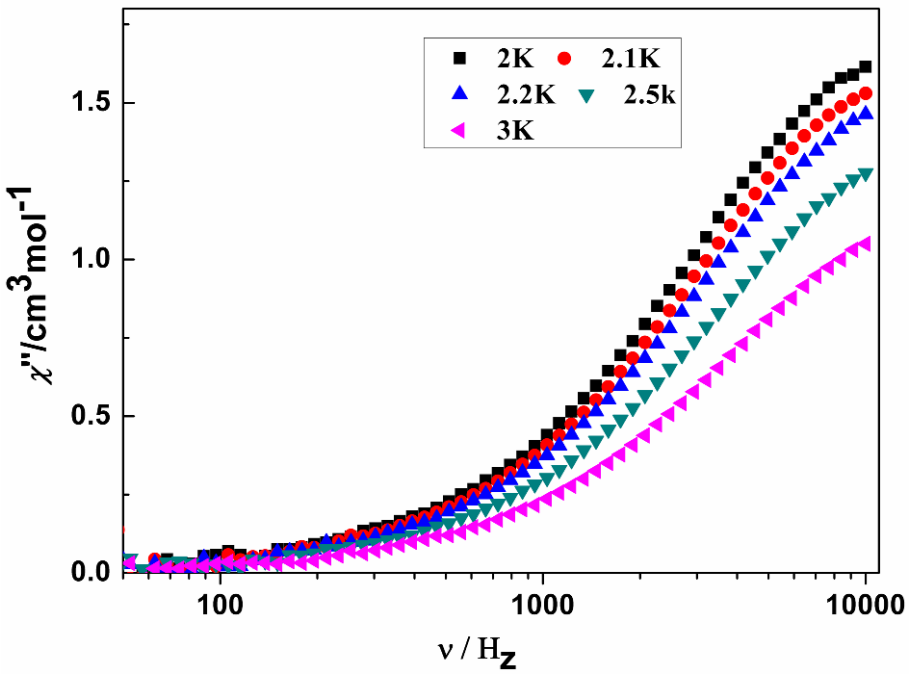

Fig. S14 Frequency dependence of the out-of-phase signals of the ac susceptibility for **1** at H_{dc} = 0 Oe.

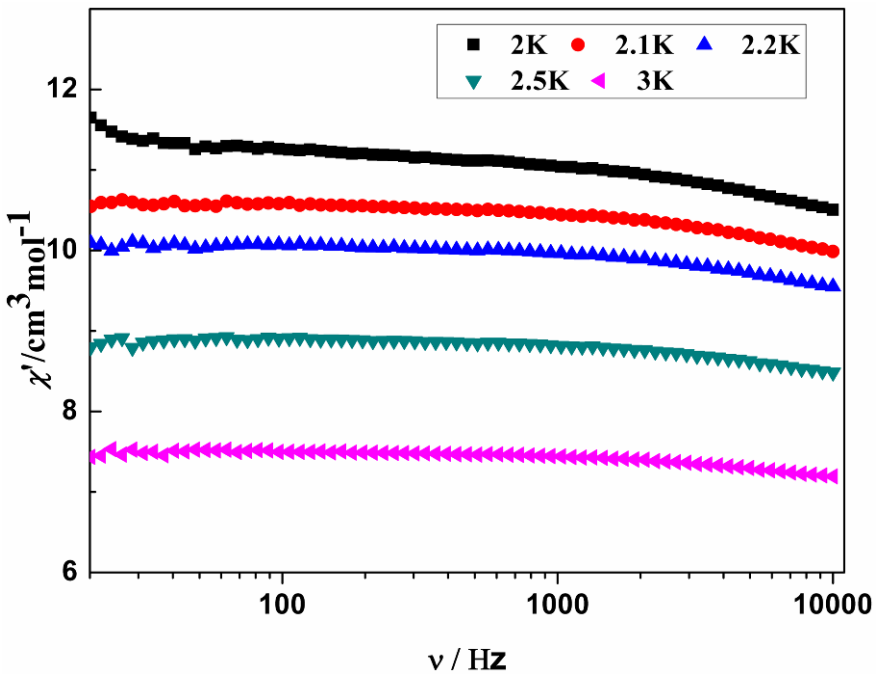

Fig. S15 Frequency dependence of the in phase signals of the ac susceptibility for **2** at H_{dc} = 0 Oe.

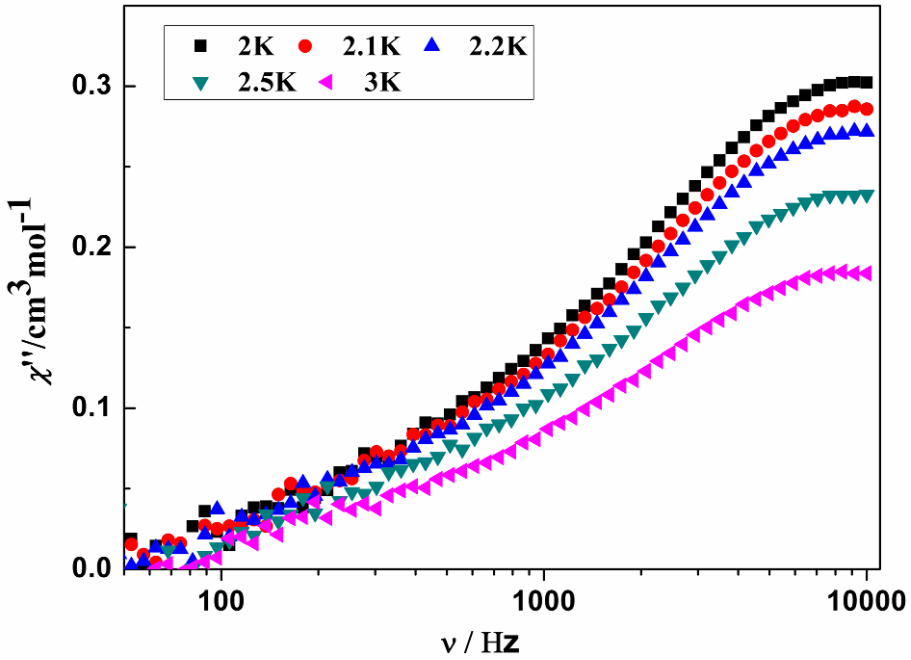

Fig. S16 Frequency dependence of the out-of-phase signals of the ac susceptibility for **2** at H_{dc} = 0 Oe.

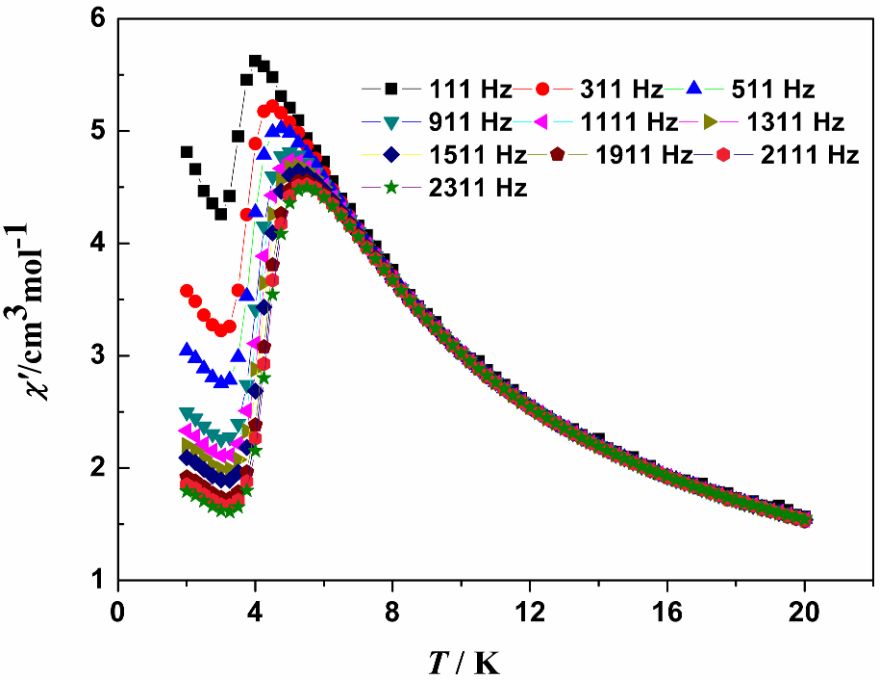

Fig. S17 Temperature dependence of the in phase signals of the ac susceptibility for **1** (H_{ac} = 3 Oe, H_{dc} = 2000 Oe). Solid lines are guides for the eye.

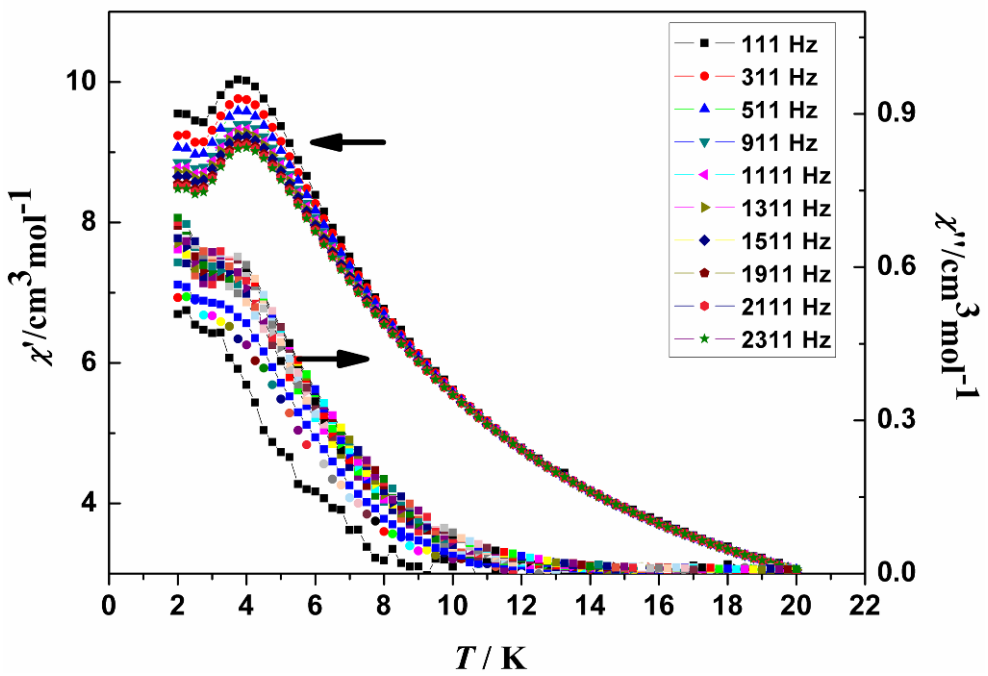

Fig. S18 Temperature dependence of the in phase and out-of-phase signals of the ac susceptibility for **2** (H_{ac} = 3 Oe, H_{dc} = 2000 Oe). Solid lines are guides for the eye.

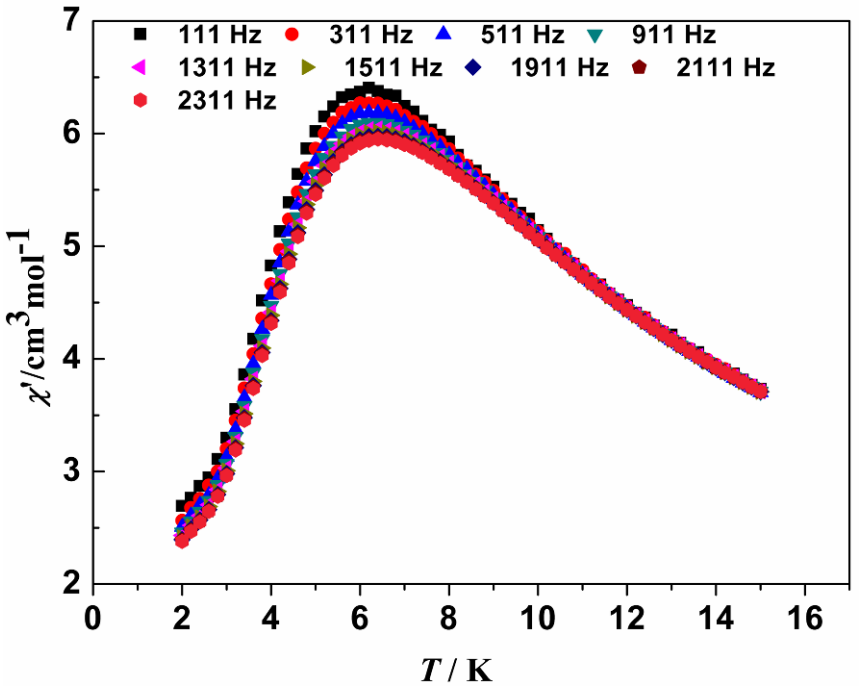

Fig. S19 Temperature dependence of the in phase signals of the ac susceptibility for **2** (H_{ac} = 3 Oe, H_{dc} = 5000 Oe).

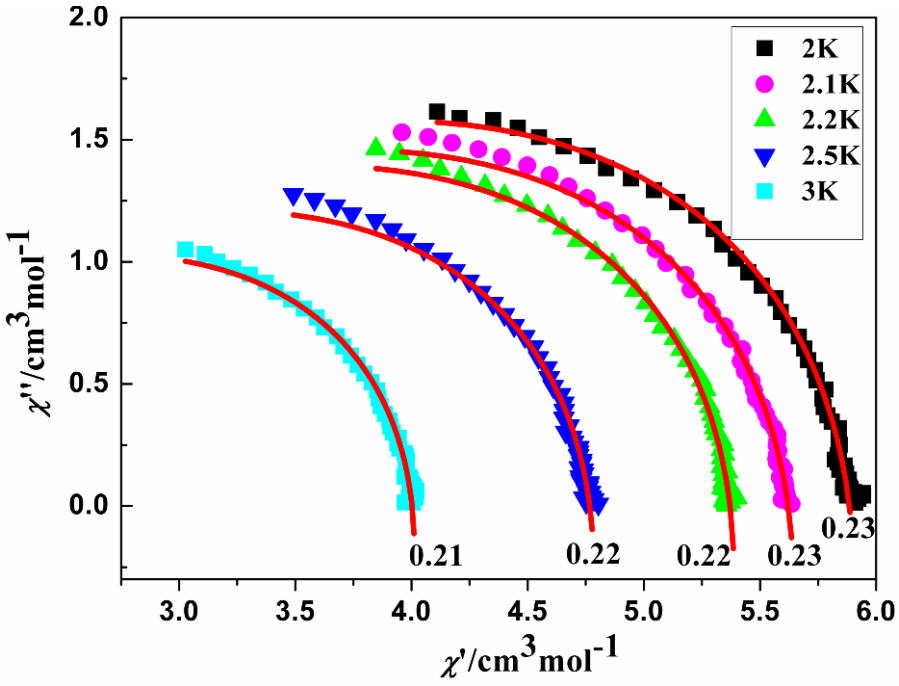

Fig. S20 Cole−Cole diagrams for **1** between 2 and 3 K at zero-dc field.

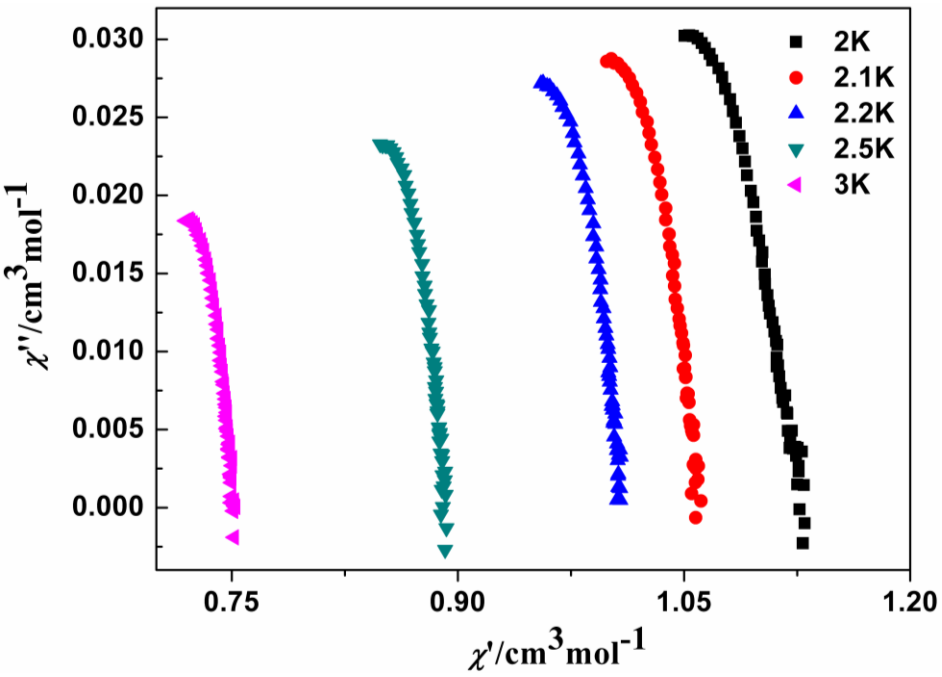

Fig. S21 Cole−Cole diagrams for **2** between 2 and 3 K at zero-dc field.

Table 1 Crystal data and structure refinement for compounds 1 and 2

Compound	**1**	**2**
Formula	$C_{24}H_{19.5}ClDyCuN_4O_{11.75}$	$C_{36}H_{50}CuDy_2N_8O_{34}$
Fw	813.43	1527.36
Crystal system	Monoclinic	Monoclinic
Space group	*C*2/c	*C*2/c
Temperature	293(2)	124.65(10)
a, Å	21.6096(5)	17.6348(11)
b, Å	12.5320(5)	16.9383(6)
c, Å	24.0555(10)	19.9934(12)
α, deg	90.00	90.00
ß, deg	116.147(2)	107.770(7)
γ , deg	90.00	90.00
V, $Å^3$	5847.9(4)	5687.2(5)
Z	8	4
Dc, g/cm^3	1.848	1.377

F(000)	3180	2260
μ, mm^{-1}	3.421	3.027
R(int)	0.0331	0.0608
Completeness/%	99.9	99.8
GOF on F^2	1.081	0.960
$R_1/wR_2(I>2\sigma(I))$	0.0322/0.0944	0.0512/0.1200
R_1/wR_2(all data)	0.0379/0.0990	0.0875/0.1339